Liquid Crystals
Publication details, including instructions for authors and subscription information:
http://www.informaworld.com/smpp/title~content=t713926090

First order transitions to a lyotropic biaxial nematic

Per-Ola Quist[a]
[a] Condensed Matter Magnetic Resonance Group, Chemical Center, University of Lund, Lund, Sweden

To cite this Article Quist, Per-Ola(1995) 'First order transitions to a lyotropic biaxial nematic', Liquid Crystals, 18: 4, 623 — 629
To link to this Article: DOI: 10.1080/02678299508036666
URL: http://dx.doi.org/10.1080/02678299508036666

LIQUID CRYSTALS, 1995, VOL. 18, NO. 4, 623–629

First order transitions to a lyotropic biaxial nematic

by PER-OLA QUIST
Condensed Matter Magnetic Resonance Group, Chemical Center,
University of Lund, P.O. Box 124, S-221 00 Lund, Sweden

(*Received 26 August 1994; accepted 27 September 1994*)

The phase diagram of the sodium dodecylsulphate/decanol/water system is studied by ^{2}H NMR spectroscopy in the range between the calamitic nematic (N_C^+) and discotic nematic (N_D^-) phases. In this narrow range a nematic biaxial phase (N_{BX}) is observed. The phase transitions between the nematic phases are all of first order. The shape of the surfactant aggregates in the nematic phases varies with composition and temperature.

1. Introduction

Amphiphilic molecules commonly self-assemble into micellar aggregates, which under certain conditions form lyotropic nematic mesophases [1–3]—anisotropic liquids consisting of micellar aggregates with long range orientational order, but no translational order. Since the first lyonematic phase was discovered in 1967 [4], three kinds of lyonematic phase have been observed—the calamitic (N_C), the discotic (N_D), and, in 1980 [5], the biaxial nematic (N_{BX}) phase. According to symmetry arguments, this represents the complete set of nematic phases [6, 7].

Until the early 1980s, the micellar aggregates in the nematic phases were believed to be very large (axial ratios in the range 10 to 20 with the minor semi-axis roughly equal to the surfactant length) [1]. Subsequent studies, however, showed that the aggregates in most systems were rather small, with axial ratios in the range 2–4 [8–12]. However, there are recent studies still showing the presence of large aggregates in some systems [13, 14].

The shape of the aggregates is still a matter of discussion. From prolate (oblate) aggregates in the N_C^+ (N_D^-) phase [1, 9] to biaxial—not only in the N_{BX} phase, but also in the N_C^+ and N_D^- phases [10, 15–17], the only difference being the long range orientational order of the micellar aggregates in the phases [10, 16]. During one period it was suggested, from theoretical considerations, that the N_{BX} phase can form from a mixture of oblate and prolate aggregates [7, 18–21]. This model has, however, been abandoned because of theoretical [22] and experimental [10, 23] results.

Until now, all three possible lyonematic phases have been observed in four surfactant systems: potassium laurate/decanol/water [5, 24], sodium decylsulphate/decanol/water [25, 26], potassium laurate/decylammonium chloride/water [27, 28], and sodium decylsulphate/decanol/water/Na_2SO_4 [26]. (A dilute N_{BX} phase was recently reported in the sodium dodecylsulphate/hexadecanol/water system [29].)

In this paper we add a fifth surfactant system to the list—sodium dodecylsulphate/decanol/water. A rough phase diagram of this system was first published in 1986 [30], but the nematic region was not discovered until 1988 [31]. Later, a more detailed phase diagram was published [32, 33].

We show that the phase transitions from the N_{BX} to the N_C^+ and N_D^- phases are first order and not second order as claimed for the potassium laurate/decanol/water system [34, 35] and inferred from Landau theory [36]. Furthermore, we show that the shapes of the aggregates, being uniaxial or biaxial, in the nematic phases change with composition and temperature. Most probably, the micellar shapes in the N_C^+, N_D^-, and N_{BX} phases vary with composition and temperature in most systems displaying lyonematic phases, and (probably) in various ways in different system [12, 14, 17].

2. Experimental

2.1. *Materials and sample preparation*

SDS (sodium dodecylsulphate, 'specially pure' grade, Merck Ltd), decanol (*n*-decanol, 'specially pure' grade, Merck Ltd) and D_2O (99·9 at.%, Sigma) were used as supplied.

Because the interesting region of the phase diagram is rather narrow, the samples were prepared in two steps. First 10 batches (*c.* 5 g each) were prepared by weighing appropriate amounts of SDS, decanol, and D_2O into glass vessels, which were sealed with a screw-cap and parafilm. The molar ratios of these samples were (approximately); $x \equiv n_{D_2O}/n_{SDS} \approx 32$ or 45 and $y \equiv n_{dec}/n_{SDS} \approx 0{\cdot}30$, 0·32, 0·35, 0·37, or 0·40 (cf. figure 2 for the exact compositions).

After thorough mixing for 3 days, the final samples were made by mixing (by weight) the desired proportions of two

0267–8292/95 $10·00

appropriate batches into Pyrex tubes, which immediately were flame-sealed. Finally, the samples were thoroughly mixed and allowed to equilibrate (at 22 ± 2°C) for 1 to 3 weeks. Some of the final samples were prepared on a later occasion from the batch samples which meanwhile had been stored at *c.* − 20°C.

To avoid effects of decomposition of the surfactant, the samples were investigated within 1 to 3 weeks after their preparation. (Samples stored at 22 ± 2°C for 2 months, showed a slightly different phase diagram.) Prior to investigation, the samples were mixed a second time and then allowed to equilibrate for 1 or 2 days.

For easy comparison with the previously published triangular phase diagrams [14, 30–33], the compositions of the investigated samples are found within the rectangular area defined by (SDS/decanol/water): (30·9/6·7/62·4), (24·6/5·4/70·0), (31·3/5·1/63·6), and (24·9/4·1/71·0) wt % (assuming the water to be a mixture of 10 wt % D_2O in H_2O [14, 32, 33]).

2.2. *NMR experiments*

The ^{2}H NMR experiments were performed using a Bruker MSL-100 spectrometer, equipped with a vertical solenoid-coil probe and a Drusch electromagnet (EAR 35N) with the horizontal field locked at 2·00 T. The sample tube was connected to a step motor (1600 steps rev^{-1}), which was controlled by the spectrometer computer. This arrangement allowed convenient angular dependent studies to be made by rotation of the sample around an axis perpendicular to the magnetic field.

The ^{2}H spectra were accumulated with a standard quadrupolar echo sequence $(90°)_x$–τ–$(90°)_{\pm y}$–τ–acq. The delay time $\tau \approx 150\,\mu$s, and the 90° pulse duration was *c.* 10 μs, the spectral width 5 kHz, and the filter width 20 kHz. The temperature was controlled by an air-flow regulator (Stelar VTC87), yielding a temperature stability of *c.* ± 0·1°C.

2.3. *Phase studies*

Prior to identification, phases were allowed to align in the magnetic field for *c.* 20 min. at 20·0°C. After each temperature change, an equilibration period of *c.* 10 min preceded the acquisition. The thermal resolution was chosen to be 1·0°C.

To distinguish between the different one-phase regions and the intermediate poly-phasic regions, we used the ^{2}H NMR spectrum of D_2O [37]. Both the aligned (no sample rotation, $\theta_{rot} = 0°$) and perpendicular (sample rotated to $\theta_{rot} = 90°$) spectra were used to identify the phase(s). The $\theta_{rot} = 90°$C spectra were recorded according to: 90° rotation (0·5 s), acquisition of 8 FIDs (15 s), 90° rotation (0·5 s). The method is similar to that used previously [5, 28].

The uniaxial lamellar phase (L_α) present in this system [32, 33] was easily identified since it does not align in the magnetic field, yielding ordinary (3D) powder spectra at both $\theta_{rot} = 0°$ and 90°. Similarly, the isotropic phase (I) yields one narrow peak at both $\theta_{rot} = 0°$ and 90°.

The nematic phases align in the magnetic field, yielding a doublet spectrum for $\theta_{rot} = 0°$ (see figure 1 (*a*)). The uniaxial N_C^+ has a positive diamagnetic susceptibility anisotropy in the director frame ($\Delta\chi_D \equiv \chi_\parallel^D - \chi_\perp^D > 0$). Therefore it aligns to a single crystal with the phase director along the magnetic field. A rotation by 90° thus yields a new doublet spectrum, but with the splitting reduced by factor 2 (see figure 1 (*b*)) [37]. (Because of the relatively high viscosity of the nematic phases, no reorientation occurs during the acquisition period of *c.* 15 s at $\theta_{rot} = 90°$.) The uniaxial N_D^- phase has $\Delta\chi_D < 0$ and aligns with the phase director perpendicular to the magnetic field. The two-dimensional distribution of the nematic director in the plane perpendicular to the magnetic field becomes visible upon rotation to $\theta_{rot} = 90°$ (see figure 1 (*c*)). The biaxial nematic phase may align with the largest component of the residual electric field gradient (efg) either along or perpendicular to the magnetic field [28]. In keeping with the notation for the uniaxial nematic phases, we shall denote these regions N_{BX}^+ and N_{BX}^-, respectively. (For comparison with figure 4 in [5], N_{BX}^+ has $\nu(90°)/\nu(0°) < 0$ while N_{BX}^- had $\nu(90°)/\nu(0°) > 0$, using their notation.)

In a biaxial phase, the singularities in the NMR spectrum occur at $\theta = 0°$ ($\theta = 90°$, $\phi = 0°$), and ($\theta = 90°$, $\phi = 90°$) [37, 38], where θ and ϕ are the Euler angles describing the orientation of the local domain with respect to the magnetic field. Depending on the distribution function $f(\theta, \phi)$, the singularities appear as peaks or shoulders, or do not appear at all in the spectrum [38]. The splittings (or shoulders) corresponding to the singularities are given by

$$\nu_Q(\theta = 0°) = \tfrac{3}{2}\langle\chi\rangle, \tag{1 a}$$

$$\nu_Q(\theta = 90°, \phi = 0°) = \tfrac{3}{4}(1 - \eta)\langle\chi\rangle, \tag{1 b}$$

and

$$\nu_Q(\theta = 90°, \phi = 90°) = \tfrac{3}{4}(1 + \eta)\langle\chi\rangle \tag{1 c}$$

where $\langle\chi\rangle$ is the motionally averaged quadrupole coupling constant and η is the asymmetry parameter of the phase. In a uniaxial phase ($\eta = 0$) the ($\theta = 90°$, $\phi = 0°$) and ($\theta = 90°$, $\phi = 90°$) singularities are degenerate.

Figures 1 (*a*) and (*d*) show the D_2O ^{2}H spectrum of N_{BX}^+ sample at $\theta_{rot} = 0°$ and 90°, respectively. In figure 1 (*d*) the three singularities can be identified, and η can be determined in two ways—either from equations (1 *a*) and (1 *b*) or from equations (1 *a*) and (1 *c*), yielding $\eta = 0{\cdot}88 \pm 0{\cdot}05$. Comparison of figures 1 (*a*) and (*d*) shows that the N_{BX}^+ samples align along the magnetic field

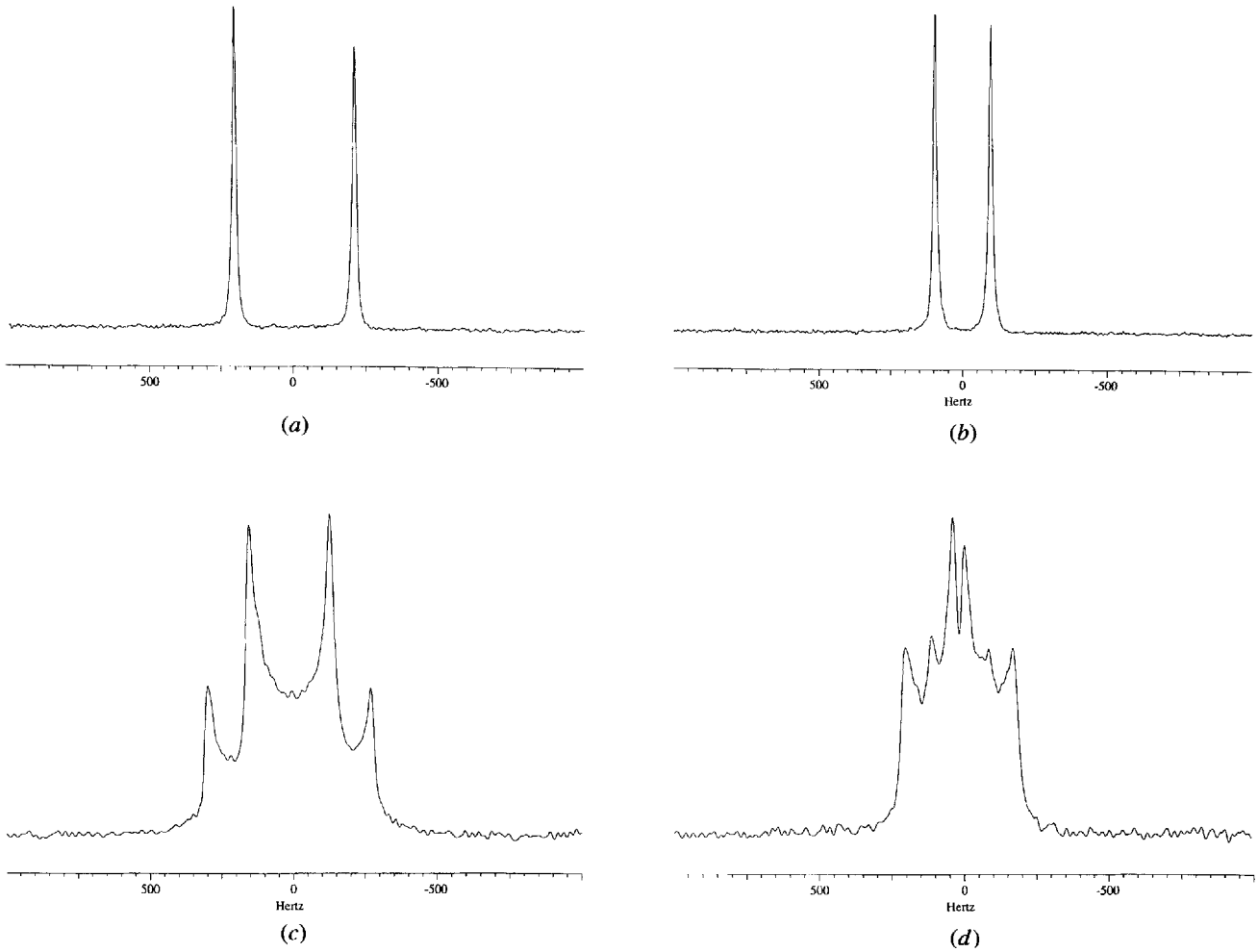

Figure 1. (*a*) D_2O ^2H NMR spectrum of an aligned nematic phase (N_{BX}^+, $x = 36{\cdot}7$, $y = 0{\cdot}324$, 20·0°C, $\theta_{rot} = 0°$). (*b*) perpendicular ($\theta_{rot} = 90°$) D_2O spectrum of an N_C^+ phase (same sample as in (*a*) but at 30·0°C), (*c*) $\theta_{rot} = 90°$ D_2O spectrum of an N_D^- phase ($x = 33{\cdot}6$, $y = 0{\cdot}324$, 20·0°C), and (*d*) $\theta_{rot} = 90°$ D_2O spectrum of the N_{BX}^+ sample in (*a*).

($\theta = 0°$). The N_{BX}^- samples, on the other hand, align with the largest residual efg component perpendicular to the magnetic field; the ($\theta = 90°$, $\phi = 90°$) singularity appears in the $\theta_{rot} = 0°$ spectrum.

The poly-phasic regions were identified as superpositions of the corresponding one-phase $\theta_{rot} = 0°$ and $\theta_{rot} = 90°$ spectra. For example, two-phase regions were easily detected by the two pairs of peaks in the $\theta_{rot} = 0°$ spectrum, and the natures of the two phases identified by comparison with the $\theta_{rot} = 90°$ spectrum.

3. Results and discussion

3.1. *The partial phase diagram*

The isothermal phase diagrams at 20·0°C and 30·0°C are shown in figure 2. The N_{BX} phase appears as two islands at 20°C, but is not found at 30°C. The extension of the N_{BX} phase appears to increase with decreasing temperature (cf. below); unfortunately, however, the SDS precipitates below *c.* 18°C.

The transition from the N_{BX} phase to the N_D^- phase is obviously first order—the samples at (x, y) = (35·2, 0·343) and (41·7, 0·358) are in a two-phase N_{BX}/N_D^- region at 20°C (see figure 2 (*a*)). The samples (40·1, 0·351) and (38·6, 0·335), on the other hand, are in a two-phase N_C^+/N_D^- region at 20°C. At 30°C the (35·2, 0·343) and (38·6, 0·335) samples are in a two-phase N_C^+/N_D^- region.

In figure 3 we show the phase diagram along the lines $y \approx 0{\cdot}324$ (see figure 3 (*a*)) and $y \approx 0{\cdot}353$ (see figure 3 (*b*)). In all the investigated N_{BX} samples, there is a first order transition from the N_{BX} phase to the N_C^+ phase on increasing the temperature. (Two superimposed spectra are observed.) Thus, the second order transitions between the N_{BX} phase and the N_C^+ or N_D^- phase observed in the potassium laurate/decanol/water system are not present in the system investigated here. Furthermore, the present system does not display a Landau point, where the N_C^+, N_D^-, N_{BX} and isotropic phases are in equilibrium (cf. figures 2 and 3).

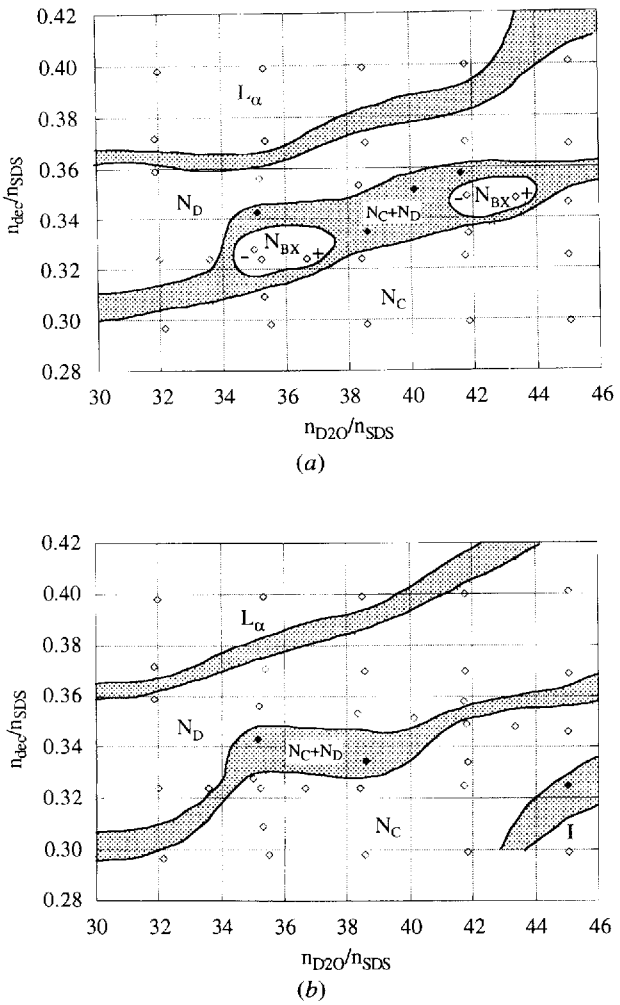

Figure 2. Isothermal phase diagram at 20·0°C (*a*) and 30·0°C (*b*). The diamonds indicate the composition of the investigation samples. Open symbols are in one-phase regions and filled symbols in two-phase regions. The '+' and '−' signs in the N_{BX} phase indicate the N_{BX}^{+} and N_{BX}^{-} regions, respectively. The shaded area indicate the approximate location of the poly-phasic regions.

From figure 3, we notice that in certain regions of the N_D^- phase, there is a first order transition to the N_C^+ phase on increasing the temperature. Such a transition also occurs for the (38·6, 0·370) and (41·7, 0·370) samples.

In most of the N_C^+ phases, there is a first order transition to the isotropic phase on increasing the temperature. The only composition (in the investigated range) where a transition from the N_D^- phase to the isotropic phase occurs is at (45·0, 0·369) and *c*. 35°C. The samples (41·7, 0·400) and (35·4, 0·371) undergo a first order transition from the lamellar L_α phase to the N_D^- phase on increasing the temperature (cf. figures 2 (*a*) and (*b*)).

For convenient comparison with the previously published phase diagrams of the present system [14, 30–33], we show in figure 4 the (partial) triangular SDS/decanol/water phase diagram at 25·0°C. The phase boundaries are established using the presently investigated samples and the determined phase boundaries in the previous studies.

3.2. *The NMR parameters*

The variation in the D_2O ^2H quadrupole splitting, ν_Q^0 (i.e. recalculated to the frame of the largest residual efg component, $\theta = 0°$), of the samples in the N_{BX} phase is shown in figure 5 (*a*). Notice the qualitatively different temperature variation in ν_Q^0 between the $N_{BX}^+ \rightarrow N_C^+$ and $N_{BX}^- \rightarrow N_C^+$ transitions—in the former case the slope of ν_Q^0 appears to vary continuously over that transition, whereas it varies discontinuously at the latter transition.

ν_Q^0 displays an unusual variation with temperature in some parts of the N_C^+ phase. After the $N_{BX}^+ \rightarrow N_C^+$ transition, $\nu_Q^0(N_C^+)$ decreases with temperature as expected [39] and commonly observed [1], whereas after the $N_{BX}^- \rightarrow N_C^+$ transition, $\nu_Q^0(N_C^+)$ passes through a maximum.

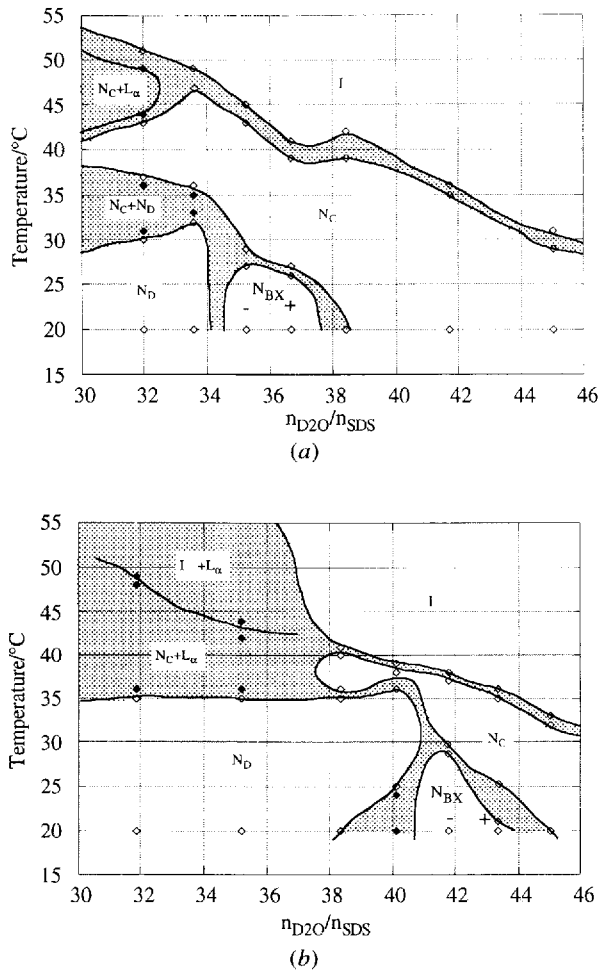

Figure 3. Partial phase diagram with $y = n_{dec}/n_{SDS} \approx 0{\cdot}324$ (*a*) and 0·353 (*b*). Same symbols as in figure 2.

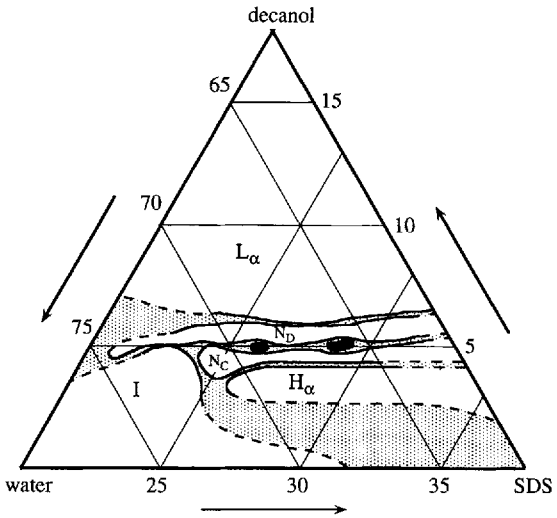

Figure 4. Partial phase diagram (in wt%) at 25·0°C. For comparison with previously published phase diagrams, the compositions of our samples are recalculated to water mixture with 10 wt % D_2O in H_2O. The phases are identified according to: I, isotropic phase: L_α, lamellar phase; H_α, hexagonal phase; N_C, N_C^+ phase; N_D, N_D^- phase. The two black areas indicate the location of the N_{BX} phase and the shaded area the poly-phasic regions.

Similar maxima in $\nu_Q^0(N_C^+)$ were observed in previous NMR studies [5, 28, 40]. We shall return to this interesting feature and show that it indicates a variation in the aggregate shape in the N_C^+ phase.

The variation in the asymmetry parameter η with temperature in the N_{BX} phase is shown in figure 5 (*b*) (for the samples with a biaxial phase). Again there is a difference between the N_{BX}^+ and N_{BX}^- samples. In the N_{BX}^+ region, η decreases with increasing temperature (as we expect, since we approach a uniaxial phase). For the N_{BX}^- samples, η increases with temperature in the vicinity of the transition to the N_C^+ phase.

3.3. *The shape of the aggregates across the N_D--N_{BX} transition*

It has been shown that the micelles in the nematic phases of the potassium laurate/decanol/water system are biaxial [10, 15, 16] and identical in all three phases—the only difference being the long range order [10, 16]. In this and subsequent sections, we show that the micellar shapes vary in the nematic phases (in the present system).

From figure 2 (*a*), it is clear that on dilution with water there is a phase sequence $N_D^- \rightarrow [N_{BX}^-$ to $N_{BX}^+] \rightarrow N_C^+$, and that on a temperature increase (see figure 3), we have the sequence $[N_{BX}^-$ or $N_{BX}^+] \rightarrow N_C^+$. Assuming biaxial aggregates of fixed shape, it is thus necessary to introduce rotational barriers to explain the differences between the phases [3, 10, 16]. In the N_D^- phase the aggregates rotate freely around the minor axis, but not around the major axis, whereas in the N_C^+ phase there is free rotation around the major axis, but not around the minor axis. In the N_{BX} phase the aggregate rotation is hindered around all axes, yielding a biaxial phase.

Dilution with water (or increasing the temperature) increases the distance between the aggregates (or increases the thermal energy) and can thus explain the transition $N_{BX} \rightarrow N_C^+$ with a fixed shape of the biaxial micelles. However, the $N_D^- \rightarrow N_{BX}$ transition observed (see figure 2 (*a*)) on aqueous dilution (observed in the present system only) cannot be explained by the model if the micelle shape is unchanged. Thus, we can conclude that the micelle shape in the N_D^- and N_{BX} phases differs—being biaxial in the N_{BX} phase and more towards the oblate limit in the N_D^- phase.

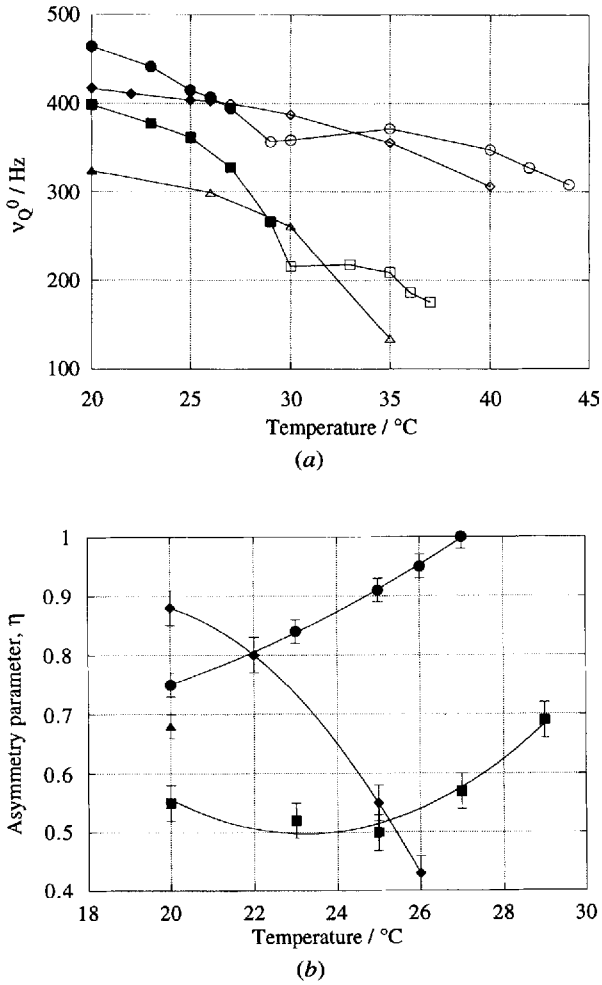

Figure 5. Temperature variation in (*a*) the ^2H_2O quadrupole splitting ν_Q^0 and (*b*) the asymmetry parameter η of the N_{BX} phase samples. Symbols: ◆ $(x, y) = (36{\cdot}7, 0{\cdot}324)$ N_{BX}^+, ▲ $(43{\cdot}4, 0{\cdot}348)$ N_{BX}^+, ● $(35{\cdot}2, 0{\cdot}324)$ N_{BX}^-, and ■ $(41{\cdot}8, 0{\cdot}349)$ N_{BX}^-. Filled symbols refer to the N_{BX} phase and open symbols to the N_C^+ phase. The lines are simply guides for the eye.

3.4. *The aggregate shape in the N_C^+ phase*

The temperature variation in the D_2O ^2H quadrupole splitting ν_Q^0 is shown in figure 5 (*a*). The variation in the quadrupole splitting with temperatures shows two types of behaviour in the N_C^+ phase: ν_Q^0 decreases smoothly with increasing temperature if the sample is in the N_{BX}^+ region at lower temperatures, or ν_Q^0 passes through a maximum with increasing temperature if the sample was in the N_{BX}^- region at lower temperatures. For comparison, ν_Q^0 decreases continuously with increasing temperature for all 17 investigated samples being in the region of the N_C^+ phase, where there are transitions to other phases than the N_{BX}^- region.

In a N_C^+ phase, ν_Q^0 depends on three parameters; the local quadrupole coupling, the shape of the aggregate, and the (restricted) aggregate tumbling [12]. In the present system and concentration region, the local quadrupole coupling for D_2O is essentially temperature independent. Since we expect an amplified (still restricted, however) aggregate tumbling on increasing the temperature [39], ν_Q^0 is expected to decrease with increasing temperature if the micellar shape is fixed. Therefore, we can conclude that the aggregate shape does change (at least) in the part of the N_C^+ phase where ν_Q^0 passes through a maximum. (In general, ν_Q^0 tends to zero on approaching spherical aggregates.) Since a maximum in $\nu_Q^0(N_C^+)$ with temperature is not unique for the present system [5, 28, 40], we can conclude that the micelle shape (in the N_C^+ phase) also varies in the potassium laurate/decanol/water and sodium decylsulphate/decanol/water systems. This conclusion is supported by recent studies of the N_D^- phase in the present system [12, 14] and of the nematic phases in the potassium laurate/decylammonium chloride/water system [17]. The shape of the micelles may, of course, be either biaxial or uniaxial.

3.5 *The aggregate shape in the N_{BX} phase*

From figure 4 (*b*), we notice that the asymmetry parameter of the biaxial phase varies not only with temperature, but also with composition. In the N_{BX}^+ region, η decreases with increasing temperature—which we expect, since the samples approach an N_C^+ phase. The decreasing η can be explained by a less restricted micelle motion or a more uniaxial-shaped aggregate, or both.

In the N_{BX}^- region, η increases with temperature in the vicinity of the N_C^+ phase. This seemingly counterintuitive behaviour can in fact be understood in terms of the progression from predominantly N_D^--like ordering towards a more N_C^+-like ordering.

From a pure NMR point of view, the theoretical treatment is identical to that for lyotropic rectangular R_x phases [38, 41, 42]—a switch of the principal frame of the residual efg from the major principal axis of the residual efg parallel (on average) to the minor axis of the aggregate to become parallel (on average) to the major axis of the aggregate [28].

The increasing η can thus be explained by a change in the aggregate shape (towards the prolate limit). This does not (necessarily) imply any dramatic changes in the aggregate shape—the biaxial micellar aggregates are (with any of the two efg principal frames), on average, oriented so as to have their major axis along the magnetic field or the minor axis perpendicular to the field. (This follows from the diamagnetic susceptibility anisotropy of the surfactants, which favours the hydrocarbon chain oriented perpendicular to the magnetic field [8, 43].) Alternatively, the increasing η in the N_{BX}^- region can be explained by a less restricted micelle motion, which makes the *effective* aggregate shape more prolate-like.

4. Conclusions

The partial phase diagram of the SDS/decanol/D_2O system is determined in the nematic region. Three nematic phases were identified—N_D^-, N_{BX}, and N_C^+. The transitions between the nematic phases (as well as to the other phases present) are first order and not second order as inferred from Landau theory.

The micelle shape in the nematic region around the N_{BX} phase in the SDS/decanol/D_2O system varies with temperature and composition. This change in interfacial curvature of the micellar aggregates is probably of similar character and magnitude to the variations of the interfacial curvature recently observed in the adjacent (defective) lamellar phase [32, 33]. The micelle shape should then change from oblate uniaxial or oblate-like biaxial (in the N_D^- phase) through biaxial micelles (in the N_{BX} phase) towards the prolate uniaxial limit (in the N_C^+) phase on aqueous dilution.

The author is grateful to Dr B. Halle for comments on the manuscript and to the Swedish Research Council for Engineering Sciences (TFR) and the Swedish Natural Science Research Council (NFR) for financial support.

References

[1] Forrest, B. J., and Reeves, L. W., 1981, *Chem. Rev.*, **81**, 1.
[2] Sonin, A.S., 1987, *Soviet Phys. Usp.*, **30**, 875.
[3] Galerne, Y., 1988, *Molec. Crystals liq. Crystals*, **165**, 131.
[4] Lawson, K. D., and Flautt, T. J., 1967, *J. Am. chem. Soc.*, **89**, 5489.
[5] Yu, L. J., and Saupe, A., 1980, *Phys. Rev. Lett.*, **45**, 1000.
[6] Freiser, M. J., 1970, *Phys. Rev. Lett.*, **24**, 1041.
[7] Rabin, Y., Mullen, W. E., and Gelbart, W. M., 1982, *Molec. Crystals liq. Crystals*, **89**, 67.
[8] Charvolin, J., Levelut, A. M., and Samulski, E. T., 1979, *J. Phys. Lett.*, **40**, L-587.
[9] Hendrikx, Y., Charvolin, J. Rawiso, M., Liebert, L., and Holmes, M. C., 1983, *J. phys. Chem.*, **87**, 3391.

[10] FIGUEIREDO NETO, A. M., GALERNE, Y., LEVELUT, A. M., and LIEBERT, L., 1985, *J. Phys. Lett.*, **46,** L-499.
[11] HOLMES, M. C., REYNOLDS, D. J., and BODEN, N., 1987, *J. phys. Chem.*, **91,** 5257.
[12] QUIST, P.-O., HALLE, B., and FURÓ, I., 1992, *J. chem. Phys.*, **96,** 3875.
[13] PHOTINOS, P., XU, S. Y., and SAUPE, A., 1990, *Phys. Rev.* A, **42,** 865.
[14] FURÓ, I., and HALLE, B., 1995, *Phys. Rev.* E, **51,** 466.
[15] HENDRIKX, Y., CHARVOLIN, J., and RAWISO, M., 1986, *Phys. Rev.* B, **33,** 3534.
[16] GALERNE, Y., FIGUEIREDO NETO, A. M., and LIEBERT, L., 1987, *J. chem. Phys.*, **87,** 1851.
[17] FORMOSO, V., GALERNE, Y., NICOLETTA, F. P., PEPY, G., PICCI, N., and BARTOLINO, R., 1993, *J. Phys. IV*, **3,** 271.
[18] ALBEN, R., 1973, *J. chem. Phys.*, **59,** 4299.
[19] CAFLISCH, R. G., CHEN, Z.-Y., BERKER, A. N., and DEUTCH, J. M., 1984, *Phys. Rev.* A, **30,** 2562.
[20] CHEN, Z.-Y., and DEUTCH, J. M., 1984, *J. chem. Phys.*, **80,** 2151.
[21] STROOBANTS, A., and LEKKERKERKER, H. N. W., 1984, *J. phys. Chem.*, **88,** 3669.
[22] PALFFY-MUHORAY, P., DE BRUYN, J. R., and DUNMUR, D. A., 1985, *J. chem. Phys.*, **82,** 5294; 1985, *Molec. Crystals liq Crystals*, **127,** 301.
[23] BASTOS DOS SANTOS, C. P., and FIGUEIREDO NETO, A. M., 1991, *Langmuir*, **7,** 2626.
[24] FIGUEIREDO NETO, A. M., LIEBERT, L., and GALERNE, Y., 1985, *J. phys. Chem.*, **89,** 3737.
[25] BARTOLINO, R., CHIARANZA, T., MEUTI, M., and COMPAGNONI, R., 1982, *Phys. Rev.* A, **26,** 1116.
[26] VASILEVSKAYA, A. S., KITAEVA, E. L., and SONIN, A. S., 1990, *Russ. J. phys. Chem.*, **64,** 599.
[27] OLIVEIRA, E. A., LIEBERT, L., and FIGUEIREDO NETO, A. M., 1989, *Liq. Crystals*, **5,** 1669.
[28] NICOLETTA, F. P., CHIDICHIMO, G., GOLEMME, A., and PICCI, N., 1991, *Liq. Crystals*, **10,** 665.
[29] HO, C. C., GOETZ, R. J., and EL-AASSER, M. S., 1991, *Langmuir*, **7,** 630.
[30] MACIEJEWSKA, D., KHAN, A., and LINDMAN, B., 1986, *Coll. Polym. Sci.*, **264,** 909.
[31] AMARAL, L. Q., and MARCONDES HELENE, M. E., 1988, *J. phys Chem.*, **92,** 6094.
[32] QUIST, P.-O., and HALLE, B., 1993, *Phys. Rev.* E, **47,** 3374.
[33] QUIST, P.-O., FONTELL, K., and HALLE, B., 1994, *Liq. Crystals*, **16,** 235.
[34] SAUPE, A., BOONBRAHM, P., and YU, L. J., 1983, *J. chim. Phys.*, **80,** 7.
[35] GALERNE, Y., FIGUEIREDO NETO, A. M., and LIEBERT, L., 1986, *J. chem. Phys.*, **84,** 1732.
[36] GRAMSBERGEN, E. F., LONGA, L., and DE JEU, W. H., 1986, *Phys. Rep.*, **4,** 195.
[37] DAVIS, J. H., 1983, *Biochim. biophys. Acta*, **737,** 117.
[38] GUSTAFSSON, S., QUIST, P.-Q., and HALLE, B., 1995, *Liq. Crystals*, **18,** 545.
[39] MAIER, W., and SAUPE, A., 1958, *Z. Naturf.* (*a*), **13,** 564; 1959, *Z. Naturf.* (*a*), **114,** 882; 1960, *Z. Naturf.* (*a*), **15,** 287.
[40] YU, L. J., and SAUPE, A., 1980, *J. Am. chem. Soc.*, **102,** 4879.
[41] CHIDICHIMO, G., VAZ, N. A. P., YANIV, Z., and DOANE, J. W., 1982, *Phys. Rev. Lett.*, **49,** 1950.
[42] QUIST, P.-O., and HALLE, B., 1988, *Molec. Phys.*, **65,** 547.
[43] LONSDALE, K., 1939, *Proc. Roy. Soc.* A, **171,** 541.